Retrieving Slowness Distribution of a Medium between Two Boreholes from First Arrival Traveltimes

D. Üstündağ

Abstract—We study a problem of reconstruction of seismic wave speed distribution from a set of measured first arrival traveltimes in presence of strong velocity contrasts, which cause the problem to be highly non-linear. In this context, we make an attempt to improve a stable iterative reconstruction algorithm by incorporating appropriate a variable regularizing parameter and also used it for a simple synthetic borehole test after writing its algorithm in a C++ code. The simulations results support the effectiveness of the method.

Keywords—Inverse Problems, Ill-Posed Problems, Nonlinear Programming, Seismic Tomography.

I. INTRODUCTİON

Tomographic analyses have been applied in many fields, with a tomography term that has been used to represent a variety of analysis procedures, the most common being medical CAT (Computerized Axial Tomography) scanning [1]-[2]. In seismic tomography[3]-[5], it refers to the measurements of arrival times of travelling seismic waves that pass through the subsurface medium. Variations in these arrival times of the seismic waves are associated with medium velocity or structure. Tomographic experiments that use these seismic wave traveltime variations to image structure of the subsurface is known more specifically as acoustic traveltime tomography. Variations on this procedure lead to the different names of tomographic applications such as attenuation tomography, waveform tomography and resistivity tomography. Most often, tomography refers to the measurements of the traveltimes differences for wave pulses transmitted through a medium and the interpreted velocity variation is associated with a physical change along the ray path as in CAT medical scans.

All tomographic techniques rely generally on the measurements of variations in some specific parameters in the medium between transmitters and receivers. So, the result is an image of physical property variation denoted as a tomogram. The objective of this paper is therefore to reconstruct the subsurface velocity structures using the principle of seismic wave propagation.

Let a seismic wave velocity $v(\mathbf{x})$ be a function of the position $\mathbf{x}$ in a medium and let $\wp$ denote all paths connecting a given source and receiver in this medium. Fermat's principle[3] states that travelling wave will take a shortest path in the medium. It actually deals with the shortest time path, which may not be straight line at all. Therefore the correct ray path between the source and receiver is the one which has the least traveltime among the others paths. Let us define τ^p to be the functional that yields the traveltime along the Fermat ray path $p \in \wp$:

$$
\begin{aligned}
\tau^p &= \Psi(v(\mathbf{x}), p) \\
&= \min_{p \in \wp} \int_p \frac{dl^p}{v(\mathbf{x})} \quad ,
\end{aligned}
\tag{1}
$$

where Ψ is a nonlinear operator and dl^p denotes the differential length along the ray path p. If more than one path produces the same minimum traveltime value, the ray path p denotes any particular member in this set. The task of tomography is thus to find a function $v(\mathbf{x})$ given the integrals τ^p over a family of manifold $\wp$. One difficulty of this approach is that the path of integration, the rays taken by seismic energy depends on the unknown velocity structure. Moreover, the ray path is required to be known in order to evaluate this integral.

Although the solution to the problem of how to reconstruct a velocity function $v(\mathbf{x})$ from the line integrals τ^p dates back to the paper by Radon[6], its applied importance has been made clear by Cormack and Hounsfield[1] in 1972. They developed an effective numerical and medical technique for exploring the interior of the human body for diagnostic purposes. Outside of the field of medicine, it has many uses including electron microscopy, acoustic and optical tomography and radio astronomy. Aki[7] was first to use seismic data in their 3-D study of the earth's crust. After this study, seismic tomography has become an important geophysical tool for producing internal structures of the subsurface using transmitted seismic waves and it has been widely studied in the literature[10]-[13].

In this work, a reconstruction method is proposed to improve on the conventional numerical algorithms by

D. Üstündağ is working at the department of mathematics, The faculty of Science and Arts, Marmara University, Göztepe Campus, Istanbul, TURKEY (email: dustundag@marmara.edu.tr).

incorporating appropriate weighting matrices and a variable regularizing parameter.

II. A MATHEMATICAL PROBLEM

The basic tomographic experiment depends on a suit of source-receiver combinations that record signals that have sampled a region of interest between two boreholes. To reconstruct subsurface velocity structure shown in Fig. 1, we first place the sources in one borehole and the receivers in the other. Secondly, we divide the rectangular region enclosed by our sources ($S_1, S_2, ..., S_m$) and receivers ($R_1, R_2, ..., R_m$) into rectangular cells of constant slowness $s(\mathbf{x})$, which is a reciprocal of wave velocity $v(\mathbf{x})$. The cells are numbered from 1 to n. Then the slowness model is defined by the vector $\mathbf{s}^T = (s_1, s_2, ..., s_n)$, where s_j represents the slowness of the jth cell. A measured data vector is defined as $\mathbf{t}^T = \{t_1, t_2, ..., t_m\}$, where the transmitter-receiver pairs and $t_i \ (i = 1, 2, 3, ... m)$ is the first arrival traveltime along the ith ray path through the medium. The superscript T represents transposing.

By using (1), in general, the relationship between $s(\mathbf{x})$ and $\mathbf{t}$ can be given in the following formula:

$$t_i = \Psi(s(\mathbf{x}), p_i) + e_i$$
$$= \min_{p_i \in \wp} \int_{p_i} s(\mathbf{x}) dl^{p_i} + e_i, \quad (2)$$

where e_i represents observation errors in the measurements. If l_{ij} is denoted as the length of the ith ray path passing through the jth cell and defined by

$$l_{ij} = \min_{p_i} \int_{p_i \cap cell\ j} dl^{p_i}, \quad (3)$$

Therefore, (2) can be reduced to a system of equations in the following form:

$$t_i = \sum_{j=1}^{n} l_{ij} s_j + e_i, \quad (i = 1, 2, ..., m). \quad (4)$$

In the vector- matrix notation,

$$\mathbf{t} = \mathbf{M}\mathbf{s} + \mathbf{e}, \quad (5)$$

where the matrix $\mathbf{M}$ is a $(m \times n)$ matrix whose entries l_{ij} are described by (3). Note that for any given ray path i, the ray path lengths l_{ij} are zero for most cells j, as the given ray path will, in general, intersect only a few of the cells in the model. This is the basic equations of forward modeling for the ray equation analysis. In other words, it can be considered as a numerical approximation to (2). Then, the mathematical problem is simply to find the slowness $\mathbf{s}$ and the ray path matrix $\mathbf{M}$ from the measurements $\mathbf{t}$. More precisely, given the first arrival data, our aim is to reconstruct the slowness distribution of the medium between boreholes shown in Fig 1.
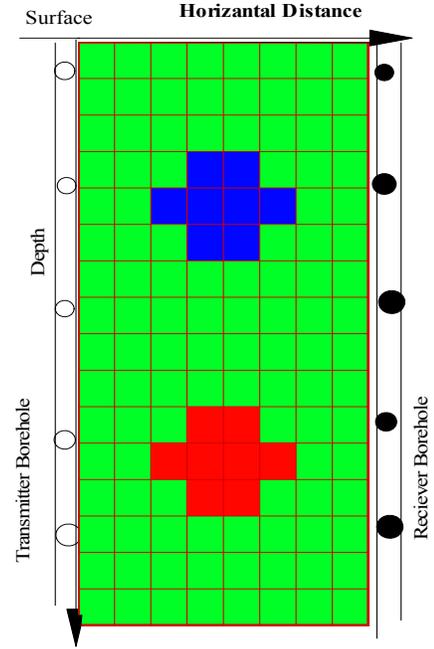

Fig. 1 simulated target slowness model of subsurface enclosed by two boreholes.

Generally, the tomographic reconstruction problem[31]-[34] is ascribed to solve a system of linear equations derived about some reference model. However, for the most tomographic problem, the ray path matrix $\mathbf{M}$ is ill-conditioned and direct solution may lead to unstable results. The system is usually ill-posed and inconsistent due to some sources of limited and noisy projection data and ray bending. Therefore, it is very important to guarantee a reasonable solution to the system equations existing at each linearized step. So, standard techniques for solving inverse problems cannot directly be applied. To stabilize the solution, some regularization schemes should be applied. A complete survey of the various regularization strategies and the available methods for the estimation of the optimal regularization parameter can be found in [14]- [20].

III. RAY TRACING

The ray tracing is based on the concept that seismic energy follows a trajectory determine by tracing equations which physically describe how energy continues in the same direction until it is refracted by the velocity variations. This is an important step for the forward problem and it is also carried in the each iteration. A good choice of ray tracing algorithm would be needed for the calculation of ray travel times between two known end points through given velocity structure and it is often called the forward modeling. Therefore, many researchers[10]-[12] have developed

different ray-tracing techniques. However, we shall only consider here to follow a bending ray method, suggested by Prothero[25], which involves bending of ray path by velocity perturbations until it satisfies a minimum traveltime criterion.
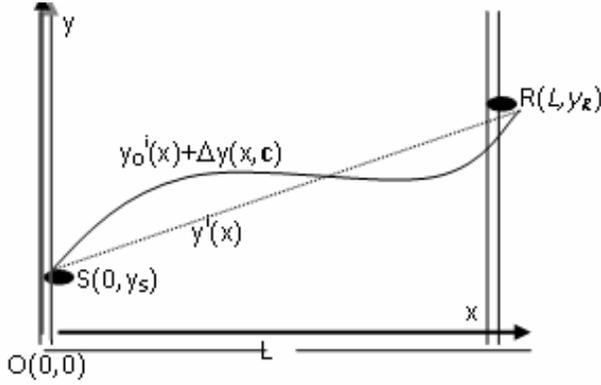

Fig 2. an illustration of ray bending

Briefly, the coordinates (x_S, y_S) and (x_R, y_R), known as a source-receiver pair respectively, are assumed to be known. The ith ray path p^i that connects the source - receiver pair shown in Fig. 2, can be found by using Fermat's principle. If the horizontal distance between two vertical boreholes is L, the initial ray path for the ith ray travelling from the source to the receiver is taken to be a straight line:

$$y_0^{\ i}(x) = (\frac{y_R - y_S}{x_R - x_S})(x - x_S) + y_S . \qquad (6)$$

The perturbation is to be a harmonic series of the form:

$$\delta y(x; \mathbf{c}) = \sum_{k=1}^{K} c_k \sin(\frac{k\pi x}{L}). \qquad (7)$$

where $\mathbf{c}^T = \{c_1, c_2, ..., c_K\}$ is a vector of the coefficients of the harmonic series. Only sine and not cosine terms are used because the end points of the ray remain unperturbed. The ith traveltime along the ith perturbed ray path, defined by

$$y^i(x; \mathbf{c}) = y_0^{\ i}(x) + \delta y(x; \mathbf{c}), \qquad (8)$$

is given by the functional:

$$\tau_i(\mathbf{c}) = \int_{x_S}^{x_R} s(x, y^i(x; \mathbf{c})) \sqrt{1 + (\frac{dy^i(x; \mathbf{c})}{dx})^2} dx . \qquad (9)$$

The problem is now reduced to the determination of the coefficients of $\mathbf{c}$ that minimise the traveltime functional τ_i :

$$min_{\mathbf{c} \in \mathfrak{R}^K} \tau_i(c_1, c_2, ..., c_K). \qquad (10)$$

The number of the coefficients in calculating the traveltime of the ray in (10) depends on the resolution of our tomographic

model. For a relatively low resolution, it is necessary to seek a general bend in rays, so we only need to determine a few coefficients of $\mathbf{c}$. However, the determination of these coefficients is difficult since they are connected nonlinearly to the traveltimes τ_i. To simplify this problem, we chose to
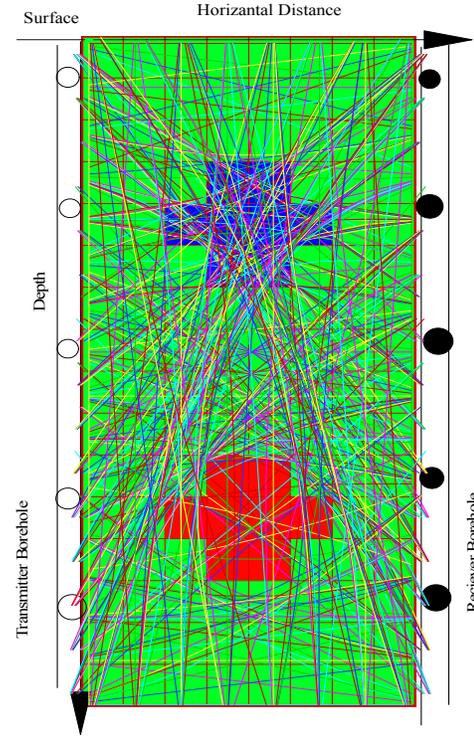

Fig. 3 mapping ray paths on the area of being imaging between two boreholes. Seismic wave escapes from low velocity regions and excites for passing through high velocity regions.

ignore the Snell's law[10] at cells boundaries and assumed that $K = 2$. Then, the problem is simply reduced to minimise the traveltime functional given in (9) with respect to two coefficients c_1 and c_2. In this context, we used a multidimensional search algorithm, which is known as the Simplex method[23]-[24] to find optimum ray paths shown in Fig. 3 for a given slowness model. Basically, starting with three points whose corresponding calculated traveltimes are τ^1, τ^2 and τ^3, respectively the algorithm seeks to replace the point with the largest traveltime by a smaller one and then other moves are made such as checking values between the original vertex and the reflected vertex or expansion (contraction) of the triangle. When an improved vertex is found, the vertices are relabelled and the process starts over for the new triangle. If no improvement (or improvement less than a preset threshold) is attained or some fixed number of iterations is executed, the process terminates for this ray path.

IV. RECONSTRUCTION METHOD

Following Berryman's works[8]-[11], the forward problem in (5) can be replaced with the feasibility constraints:

$$(\mathbf{Ms})_i \geq t_i, \quad (i = 1, 2, ..., m). \tag{11}$$

This arises from Fermat's principle and implies that the first arrival rays follow the path with a minimum traveltime for a given model $\mathbf{s}$. Thus, if $\mathbf{s}$ is a true model then any ray path matrix $\mathbf{M}$ must satisfy these constraints. Therefore, any model that violates the constraints in (11) along any ray path matrix $\mathbf{M}$ is called a nonfeasible set. Moreover, for the m-feasible constraints the limiting equality is an equation for the hyperplane in the n-dimensional model space. The feasible region is therefore bounded by these hyperplanes and by the planes determined by the constraints from the positivity of slowness in all cells,

$$s_j > 0, \quad (j = 1, 2, 3, ..., n). \tag{12}$$

It can easily be shown that the constraints in (11) and (12) imply that the feasible region of the model space is convex. Hence, for a fixed ray path matrix $\mathbf{M}$ the set of all feasible models includes models either inside of the feasible region or on the feasibility boundary determined by $\mathbf{M}$ and $\mathbf{t}$. For any combination of the ray-path matrix $\mathbf{M}$, slowness vector $\mathbf{s}$ and the measured traveltimes $\mathbf{t}$, the number of rays violating those constraints in (11) can easily be calculated and it is called the feasibility violation number (fvn), determined by

$$fvn(\mathbf{s}) = \sum_{i=1}^{m} \delta\left[t_i - (\mathbf{Ms})_i\right], \tag{13}$$

where the step function δ is defined by

$$\delta(x) = \begin{cases} 1 & x > 0 \\ 0 & x \leq 0 \end{cases}. \tag{14}$$

Following Lanczos[12], a generalized eigenvalue problem with the appropriate weighting matrices can be implemented in the form:

$$\begin{bmatrix} 0 & \mathbf{M} \\ \mathbf{M}^T & 0 \end{bmatrix} \begin{bmatrix} \mathbf{u} \\ \mathbf{v} \end{bmatrix} = \begin{bmatrix} \mathbf{L} & 0 \\ 0 & \mathbf{C} \end{bmatrix} \begin{bmatrix} \mathbf{u} \\ \mathbf{v} \end{bmatrix}, \tag{15}$$

where $\mathbf{u}$ and $\mathbf{v}$ are m and n vectors of ones, respectively. The matrix on the right is defined in terms of diagonal matrices $\mathbf{L}$ and $\mathbf{C}$, whose diagonal elements are the row sum L_i and the column sum C_j of the matrix $\mathbf{M}$, respectively. The quantity L_i is the total length of the ith ray path. The quantity C_j is the total ray path segments passing through the jth cell. It is called the coverage of cell j. Any cell with $C_j = 0$ is uncovered and therefore lies outside the span of the data for the current choice of ray paths. We retain only covered cells in the reduced slowness vector $\widetilde{\mathbf{s}}$ with $\tilde{n} \leq n$.

By deleting the corresponding columns in the matrix $\mathbf{M}$, the size of the ray path matrix $\mathbf{M}$ is thus reduced. For the simplicity, we assumed $\widetilde{n} = n$ in the following discussions.

In agreement with Berryman[4], an analogous to the eigenvalue problem[21] providing for high contrast reconstruction can be given in the following form:

$$\begin{bmatrix} 0 & \mathbf{M} \\ \mathbf{M}^T & 0 \end{bmatrix} \begin{bmatrix} \mathbf{w}_\lambda \\ \mathbf{x}_\lambda \end{bmatrix} = \lambda \begin{bmatrix} \mathbf{T} & 0 \\ 0 & \mathbf{D} \end{bmatrix} \begin{bmatrix} \mathbf{w}_\lambda \\ \mathbf{x}_\lambda \end{bmatrix}, \tag{16}$$

where for $\lambda = 1$, $\mathbf{w}_1 = \mathbf{u}$, $\mathbf{x}_1 = \mathbf{s}$ and the diagonal weighted matrices are as follow

$$\mathbf{T} = \mathbf{L}\mathbf{s} \text{ and } \mathbf{D} = \mathbf{C}\mathbf{s}^{-1}. \tag{17}$$

By writing (15) in the canonical form, we get

$$\begin{bmatrix} 0 & \mathbf{A} \\ \mathbf{A}^T & 0 \end{bmatrix} = \begin{bmatrix} \mathbf{T}^{\frac{-1}{2}} & 0 \\ 0 & \mathbf{D}^{\frac{-1}{2}} \end{bmatrix} \begin{bmatrix} 0 & \mathbf{M} \\ \mathbf{M}^T & 0 \end{bmatrix} \begin{bmatrix} \mathbf{T}^{\frac{-1}{2}} & 0 \\ 0 & \mathbf{D}^{\frac{-1}{2}} \end{bmatrix}$$
$$= \begin{bmatrix} 0 & \mathbf{D}^{\frac{-1}{2}}\mathbf{M}\mathbf{T}^{\frac{-1}{2}} \\ \mathbf{T}^{\frac{-1}{2}}\mathbf{M}^T\mathbf{D}^{\frac{-1}{2}} & 0 \end{bmatrix} \tag{18}$$

and

$$\begin{bmatrix} \mathbf{y} \\ \mathbf{z} \end{bmatrix} = \begin{bmatrix} \mathbf{T}^{\frac{1}{2}}\mathbf{u} \\ \mathbf{D}^{\frac{1}{2}}\mathbf{s} \end{bmatrix} \tag{19}$$

Thus, the problem given in (16) can be transformed[33] into the following form:

$$\begin{bmatrix} 0 & \mathbf{A} \\ \mathbf{A}^T & 0 \end{bmatrix} \begin{bmatrix} \mathbf{y} \\ \mathbf{z} \end{bmatrix} = \begin{bmatrix} \mathbf{y} \\ \mathbf{z} \end{bmatrix} \tag{20}$$

As we have seen above, with normalisation the current slowness model $\mathbf{s}$ gives rise to the unique eigenvector with the highest eigenvalue and that eigenvalue is unity. Given a set of transmitter-receiver pairs and any model slowness $\mathbf{s}$, Fermat's principle can then be used to find the ray-path matrix $\mathbf{M}$ associated with $\mathbf{s}$ and with any slowness $\gamma\mathbf{s}$ ($\gamma > 0$) in the same direction as $\mathbf{s}$. If the normalised data is given by

$$\mathbf{y} = \mathbf{T}^{\frac{-1}{2}}\mathbf{t} \tag{21}$$

then the first problem is to find a value of γ such that the following functional

$$\phi(\gamma) = (\mathbf{y} - \mathbf{A}\gamma\mathbf{z})^T(\mathbf{y} - \mathbf{A}\gamma\mathbf{z}), \tag{22}$$

achieves its minimum at the value:

$$\gamma = \frac{\mathbf{z}^T\mathbf{A}^T\mathbf{z}}{\mathbf{z}^T\mathbf{A}^T\mathbf{A}\mathbf{z}} = \frac{\mathbf{z}^T\mathbf{A}^T\mathbf{y}}{\mathbf{z}^T\mathbf{z}}. \tag{23}$$

Because $\mathbf{A}^T\mathbf{A}\mathbf{z} = \mathbf{z}$. Having found optimal slowness $\mathbf{s}_\gamma = \gamma\mathbf{s}$ in the given direction $\mathbf{s}$, the second problem is to find another direction in the slowness vector space that gives better fit to the measured traveltimes by minimizing the following functional:

$$\varphi(\mathbf{z},\mu) = (\mathbf{y}-\mathbf{A}\mathbf{z})^T(\mathbf{y}-\mathbf{A}\mathbf{z}) + \mu(\mathbf{z}-\mathbf{z}_\gamma)^T(\mathbf{z}-\mathbf{z}_\gamma), \qquad (24)$$

where μ is a regularizing parameter and controls the relative importance between the constrained norm $\|\mathbf{z}-\mathbf{z}_\gamma\|_2$ and residual norm $\|\mathbf{y}-\mathbf{A}\mathbf{z}\|_2$. The minimum of (24) occurs at

$$\mathbf{z}_\mu = \arg\min_{\mathbf{z}\in\mathfrak{R}^n} \varphi(\mathbf{z},\mu), \quad \mu > 0 \qquad (25)$$

where $\mathbf{z}_\mu$ satisfies the following system of the linear equations:

$$\left(\mathbf{A}^T\mathbf{A} + \mu\mathbf{I}\right)(\mathbf{z}_\mu - \mathbf{z}_\gamma) = \mathbf{A}^T\mathbf{y} - \mathbf{z}_\gamma. \qquad (26)$$

So long as the matrix $(\mathbf{A}^T\mathbf{A} + \mu\mathbf{I})$ for any $\mu > 0$ is non-singular, there is a unique solution. Hence, the problem is reduced to solve a (large) system of simultaneous equations with a symmetric positive definite coefficient matrix. For each iteration, the conjugate-gradient (CG) algorithm[24], which is known as one of the most effective algorithm can successfully be applied to solve the resulting set of linear equations in (26) for $\mathbf{z}_\mu$ for a given μ . It is terminated when the relative change in the solution is less than 0.001%. What makes the conjugate gradient method so effective, especially for sparse problems, is that the matrix appears only through matrix-vector products, and the search vectors are also calculated recursively and not stored.

The big question now is "how to choose the regularizing parameter μ"? If μ is chosen to be too small the reconstruction is dominated by large, high frequency noise components. If μ is chosen to be too large the effect of the regularization term will dominate the solution and important information in the data will be lost. Many approaches to choosing an appropriate value for μ have been presented in the literature by different researchers [26]-[30]. Of particular interest for this work are methods based on what is called the L-curved. Briefly, when we plot the logarithmic value of semi norm $\|\mathbf{s}_\mu - \mathbf{s}_\gamma\|_2$ versus the logarithmic value of $\|\mathbf{d}-\mathbf{M}\mathbf{s}_\mu\|_2$ we get the characteristic L-shaped curve with a (often) distinct corner separating vertical and horizontal parts of the curve. In the vertical part of the curve the solution semi norm is a very sensitive function of the regularization parameter because the solution is undergoing large changes with μ , in an attempt to fit the data better. On the horizontal part, the solution is not changing very much as μ is changed. So it is desirable to choose a solution which lies not too far to the right of the corner. However, computation of the L-corner requires many repeated solutions of the corresponding regularization problem for different values of μ , a potentially very costly task.

Therefore, an alternative criterion is that the value of μ is chosen so as to place the solution on the edge of the set as defined by a Chi-squared statistics[27] $\chi^2(\mathbf{s}_\mu) \leq \chi^2_0$. The value of χ^2_0 is selected such that the probability of exceeding this value due to chance alone is smaller than some threshold, say one percent. However, an inaccurate characterization of the forward problem in the ray tracing process can sometimes lead to under-regularization.

Another point $\mathbf{s}_\mu = \mathbf{D}^{-\frac{1}{2}}\mathbf{z}_\mu$ in the slowness vector space can thus be obtained. Although the point $\mathbf{s}_\mu$ gives a better fit to travel time data, this fit is certainly spurious to some extent because it is based on the wrong ray path matrix $\mathbf{M}$ used in the computation of $\mathbf{s}_\mu$. Thus, both of the points we have found, lie in the nonfeasible part of the vector space. If the solution of (5) exists, in agreement with Berryman, it must lie on the boundary of the feasible region. So $\mathbf{s}_\gamma$ and $\mathbf{s}_\mu$ may be used to find an optimum point on this boundary in the sense that it is as consistent as possible with the ray path matrix, with the travel time measurements and with the feasibility constraints. Because of the convex property of the feasible region, there exists a point $\mathbf{s}$ between points $\mathbf{s}_\gamma$ and $\mathbf{s}_\mu$ that
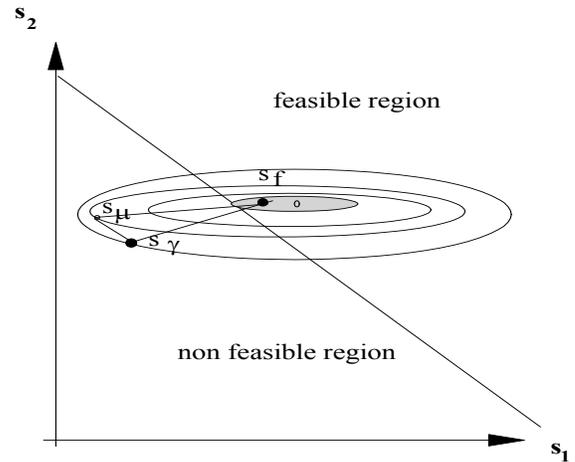

Fig. 4 stopping criterion of the algorithm.

is closer to the feasible region than the either of two end points. This can easily be found by computing the feasibility violation number and choosing the model that gives a minimum violation number[6]-[14] when we move in the direction $(\mathbf{s}_\mu - \mathbf{s}_\gamma)$ from $\mathbf{s}_\gamma$. Then, we get

$$\hat{\mathbf{s}} = \mathbf{s}_\gamma + \alpha(\mathbf{s}_\mu - \mathbf{s}_\gamma). \qquad (27)$$

As α gets smaller, it is expected that the inversion method is not providing any further improvement so that a threshold for α of 0.25 is used to stop searching. Once we find $\hat{\mathbf{s}}$ and then scale it up to the point, denoted as $\mathbf{s}_f$ in the same

direction lying in the feasibility boundary. It is not hard to see that these three points $\mathbf{s}_\gamma$, $\mathbf{s}_\mu$ and $\mathbf{s}_f$ are distinct unless we found the exact solution of the inverse problem in (5). Otherwise, these three points, shown in Fig 4 form a triangle and its area may give us an estimate how far we are from the solution.

Finally, the iterative reconstruction algorithm that uses the above ideas is thus coded by using C++ programming language and tested for artificially generated traveltime data. The results are given in the following section.

V. COMPUTER SIMULATIONS

For a comparison with Berryman' results, we took a similar model slowness structure shown in Fig. 5(a). Two boreholes on either side of the region contain an array of seismic sources and receivers and the region of imaging is divided into (8×16) cells. In according to Berryman, both on the upper half and the lower half of the medium there is a cross anomaly area respectively. The slowness of the upper anomaly area is larger than the background slowness and the slowness of the lower anomaly area is less than the background slowness. If the background slowness is taken as one, we then parameterised the model slowness by β, where the slow region had a slowness of $1 + \beta$ and the fast region had a slowness of $1 - \beta$ $(\beta = 0.2, 0.5)$. Thus, variations in the value of β will provide variations in the contrast of the model slowness. We first chose $\beta = 0.2$ for the low contrast and generate the traveltime data by using the ray tracing method described in the paper. As mentioned before, the simplex ray path is constrained by the use of two coefficients in the sine series expansions to be quite smooth, perhaps smoother than it should be for such high contrast media. Traveltime data, shown in Fig 5(b), consists of 320 rays, including 256 (16×16) rays travelling from left to right and 64 (8×8) rays travelling from bottom to top. Given the first arrival time data in Fig 5(b), our aim is to reconstruct the velocity structure between the boreholes. To achieve this, our computer program was run on a Pentium IV personal computer (P.C.). The results, shown in Fig. 5(c)-(f) illustrate the convergence of the method. It can be seen that as the number of iterations increases, the fast anomaly is reconstructed very well while the slow anomaly is located well. As β increases we get higher contrast and expect that the slow anomaly could always be harder to reconstruct because few or no first arrivals pass through this region. We therefore chose $\beta = 0.5$ for the high contrast and generated the traveltime data by using the ray tracing method. This is illustrated in Fig. 6. For small contrast (less than 20%), the method produces uniformly excellent results even though the data contain zero-mean random noise with a variance less
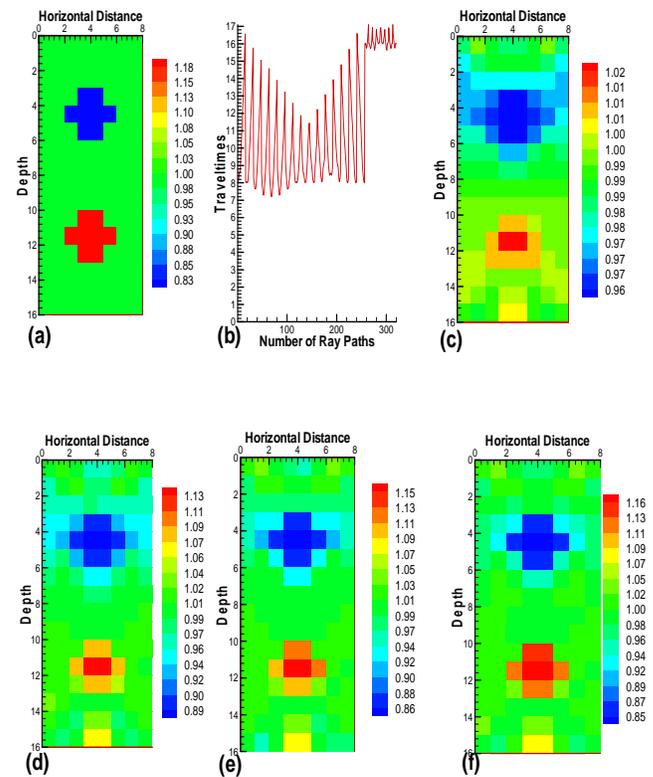

(a) (b) (c)

(d) (e) (f)

Fig. 5 (a) slowness model having contrast with 20% anomaly. (b) Traveltime data. Reconstructions obtained at (c) the first, **(d)** 10th, (e) 20th and (f) 30th iterations by the method given in this paper.
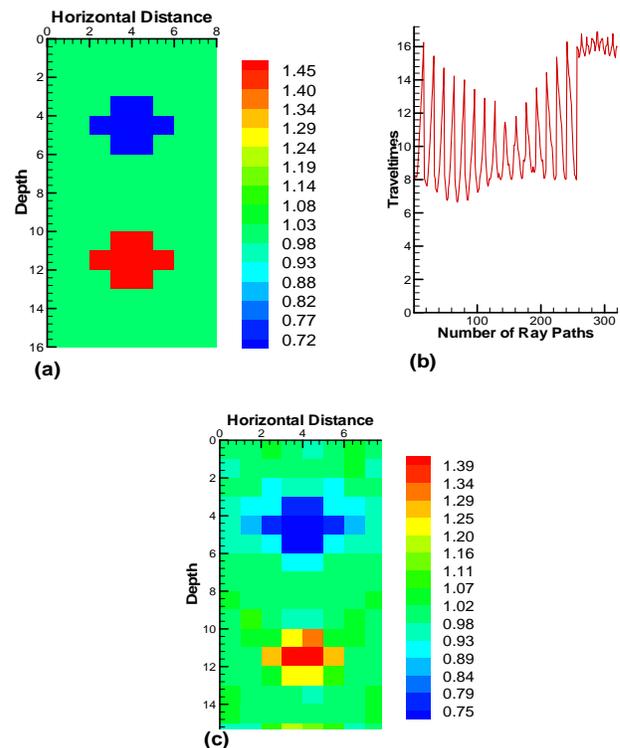

(a) (b)

(c)

Fig. 6 (a) slowness model having contrast with 50% anomaly. (b) Traveltime data. (c) Reconstructed slowness distribution.

than 0.01. For large contrast, it becomes less accurate. However, experimental results show that the reconstructed slowness models obtained are closer to the target slowness than the obtained by the use of the damped least squared method ($\mu = 1$). The method converges quite rapidly to a definite result unless we force the algorithm to make a minimum percentage correction step per iteration as 1-10% of the distance along the direction $(\mathbf{z}_\mu - \mathbf{z}_\gamma)$. In an agreement with Berryman, it requires at least 10 iterations for getting reasonable results.
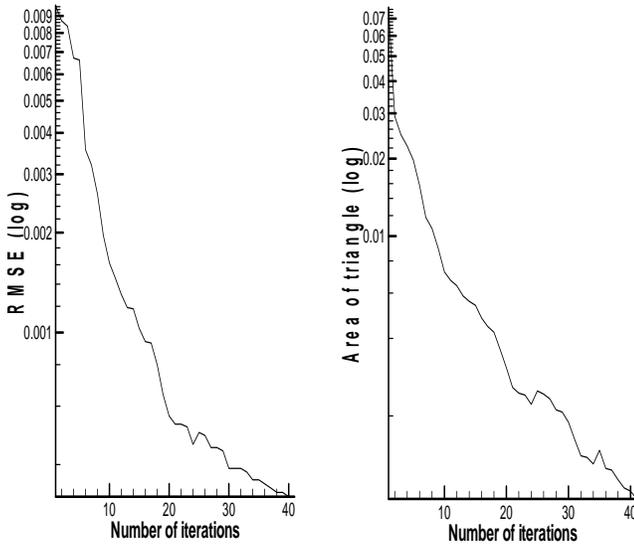

Fig. 7 area of triangle used as a stopping criterion for the algorithm and the root mean square error versus with the number of iterations.

Variations in the stopping criterion used in the algorithm with respect to the number of iterations are shown in Fig. 7. It is clearly seen that as the number of iterations increases, the area of triangle decreases monotonically and subsequently oscillates around a small number. On the other hand, a quantitative measure of the improvement appears in Fig 7, which plots reconstruction error[1] as a function of the number of iterations. It can be seen that the reconstruction error first decreases rapidly and then reduces gradually as the number of iteration increases.

Finally, we assume that a medium between two boreholes, shown in Fig. 8(a), consists of horizontal layers with the randomly chosen velocities at the different levels of depth. Then, we perform the same experiment to obtain the traveltime data in Fig. 8(b). By using this data, we ran our computer program on the Pentium IV P.C. and got the result shown in Fig 8(c). It is clearly seen that horizontal layers with velocities are estimated with an error of a few percent and the boundaries of the layers are almost recovered well.

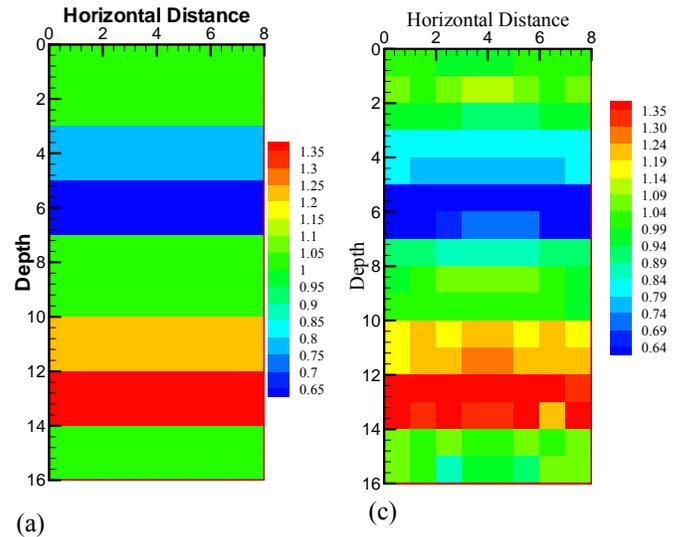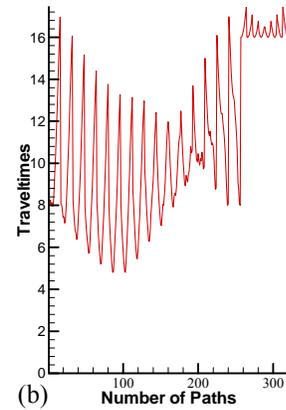[1] $rmse = \sqrt{\dfrac{1}{m}\sum_{i=1}^{m}(t_i - \hat{t}_i)^2}$

Fig. 8(a) slowness model varying randomly at the different depths. (b) Traveltime data. (c) Reconstructed slowness distribution after 30 iterations.

VI. CONCLUSION

The results presented here are encouraging us for retrieving the slowness distribution of a medium from the first arrival traveltimes, which contain the errors made by neglecting ray bending effects far more significant than measurements errors. Even if the data contain errors less than 1%, it gives very stable reconstructions and avoids the large oscillations often found in traditional least squared methods. Although Fermat's principle determines the ray path matrix once slowness is given, it also determines which slowness vectors are feasible and infeasible. Therefore, this plays an essential role in the reconstruction algorithm when the data have no noise. On the other hand, it requires a large consumption of computer time because of the computation of the ray path matrix. This can be reduced by using parallel processing techniques because each ray path may be computed independently of the others. If we incorporate into above analysis any other geophysical information as constraints to guide the imaging or inversion, we could get more improvement in the reconstruction. In this context, Bayesian methodology combined with Markov Chain

Monte Carlo techniques could be more appropriate for this kind of problems. Therefore, it deserves further investigation.

REFERENCES

[1] G.T. Herman, *Image Reconstruction from Projection- the Fundamentals of Computerized Tomography*, New York: Academic, 1980.

[2] R. A. Brooks and G. DiChiro, "Principles of computer assisted tomography (CAT)in radiographic and radio isotopic imaging," *Physical Medical Biology*, Vol. 21, 1976, pp. 689-732.

[3] W.H.K. Lee and V. Pereyra, "*Seismic tomography /theory and practice,*" H.M Iyer & K. Hirahara eds., Chapman & Hall, London, 1993, pp. 9-21.

[4] K. A. Dines and R. J. Lytle, "Computerized geophysical tomography," in proc. *of IEEE*, 1979, vol. 67, pp. 1065–1072.

[5] S. Ivansson, "Seismic Borehole Tomography-theory and computational methods," in *Proc. IEEE*, Vol. 74, 1986, pp. 328–338.

[6] J. Radon,"Über die bestimmung von funktionen durch ihre integralweite langs gewisser mannigfaltigkeiten," *Ber. Verh. Saechs. Akad. Wiss, Leipzig. Mathematical Physic*s, vol. 69, 1917, pp. 262-277.

[7] K. Aki and W.H.K. Lee, "Determination of three dimensional velocity anomalies under a seismic array using first P-arrival time from local earthquakes:1.a homogeneous initial model," *Journal of Geophysics Researches*, vol. 81, 1976, pp. 4381-4399.

[8] J.G Berryman, "Fermat's principle and nonlinear tomography," *Physical Review Letter, vol. 62*, 1989, pp. 2953-2956.

[9] J.G. Berryman, "Stable Iterative Reconstruction Algorithm for Nonlinear Traveltime Tomography," *Inverse Problems, v*ol. 6, 1990, pp. 21-42.

[10] J.G. Berryman, *Lecture Notes on Nonlinear Inversion and Tomography.* Earth Resources Laboratory, Massachusetts Institute of Technology, USA, 1991.

[11] J.G. Berryman, "Global extrema in traveltime tomography," *in Computational Acoustics, vol. 2,* D. Lee, R. Wichinevetsky and A.R. Rabinson Eds. 1993, pp.45–62.

[12] Bo´na and M.A. Slawinski, "Ray paths as parametric curves in anisotropic, nonuniform Media: differential-geometry approach," *Nonlinear Analysis*, vol. 51, 2002, pp. 983-994.

[13] M. Bosch, R. Barton, S.C. Singh and I. Trinks, "Inversion of traveltime data under a statistical model for seismic velocities and layer interfaces," *Geophysics*, vol. 70, 2005, pp.33-43.

[14] H.W. Engl, M. Hanke, A. Neubauer, "*Regularization Inverse Problems,*" Kluwer Academic Publishers, Dordrecht, The Netherlands, 1996.

[15] P. C. Hansen, "Regularization tools: A Matlab package for analysis and solution of discrete ill-posed problems," *Numerical Algorithms*, vol. 6, 1994, pp. 1-35.

[16] N. Tikhonov and V. Y. Arsenin, *Solution of Ill-Posed Problems.* New York: Wiley, 1977.

[17] D. Üstündağ, N.M. Queen, G.K Skinner and J.E. Bowcock, "Two new methods for retrieving an image from noisy incomplete data and comparison with the Cambridge MaxEnt package," in *Maximum Entropy and Bayesian Methods,* W.T. Grandy, Jr. and L.H. Schick Eds. Kluwer Academic Publisher, 1991, pp.295-301.

[18] D. Üstündağ, N.M. Queen and J.E. Bowcock, "A method for retrieving Images from Noisy Incomplete Data, *Proceedings of the fifth Alvey Vision Conference*, 1989, pp. 239-244.

[19] D. Üstündağ, E. Ozbasaran, "Recovering images from traveltime data," *Mathematical and Computational Applications*, vol. 8, 2003, pp. 95-102.

[20] D. Üstündağ and M. Cevri," Estimating Parameters of Sinusoids from Noisy Data Using Bayesian Inference with Simulated Annealing," *Wseas Transaction on Signal Processing*, vol. 7, 2008, pp. 432-442.

[21] C. Lanczos, "An iteration method for the solution of the eigenvalue problem of linear differential equations and integral operators," *J. Res. National Bureau Standards, v*ol. 45, 1950, pp. 255-282.

[22] D.W. Marquardt, "Generalized inverses, ridge regression, biased linear and nonlinear estimation," *Technometrics*, vol. 12, 1970, pp. 591-592.

[23] J.A. Nelder and R. Mead, " Simplex method for function minimization," *Computer Journal, v*ol. 7, 1965, pp. 308-313.

[24] W.H. Press, B.P. Flannery, S.A. Teukolshy and W.T. Vetterling, *Numerical Recipes in C: The Art of Computing.* Cambridge University Press, 1995.

[25] W.A. Prothero, W.J. Taylor and J.A. Eickemeyer, " Fast two-point, three-dimensional ray tracing algorithm using a simple search method," *Bulletin of Seismological Society America*, vol. 78, 1988, pp.1190-1198.

[26] R. Penrose, "Generalized inverse for matrices," in *Proc. Cambridge Philosophical Society, v*ol. 51, 1955, pp. 406-413.

[27] V. A. Morozov, *Methods for Solving Incorrectly Posed Problems*, Springer Verlag, New York, 1984.

[28] K.E. Atkinson, A*n Introduction to Numerical Analysis*. Wiley, New York, USA, 1997.

[29] Van der Sluis and H. A. Van der Vorst, "Numerical solution of large sparse linear algebraic systems arising from tomographic problems", in *Seismic Tomography,* G. Nolet. Ed. Dordrecht, The Netherlands: Reidel, 1987, pp. 49–84.

[30] J. A. Scales, "Tomographic inversion via conjugate gradient method," Geophysics, vol. 52, 1987, pp. 159-185.

[31] J. A. Scales and R. Snieder, "The anatomy of inverse problems.," *Geophysics*, vol. 6, 2000, pp. 1708-1710.

[32] A. Tarantola, *Inverse Problem Theory: Methods for Data Fitting and Model Parameter Estimation.* Society for Industrial and Applied Mathematics, New York, 1991.

[33] Li Shuhong, Li Jing, Xing Gao, "Digital image scrambling approaches using multi-dimensional orthogonal transform and fast realization**,"** *Wseas Transaction on Signal Processing* , vol. 3, 2007, 459–466.

[34] K. Teimoornegad and N. Poroohan, "Application of Seismic Tomography Techniques in Dam Site," *Wseas Transactions on Signal Processing,* vol. 4, 2008, pp.825-835.